DTIC FILE COPY

AD-A198 255

(4)

REPORT DOCUMENTATION PAGE

Form Approved OMB No. 0704-0188

DTIC ELECTE JUL 20 1988 S D

1a. REPORT SECURITY CLASSIFICATION NONE	1b. RESTRICTIVE MARKINGS NONE
2a. SECURITY CLASSIFICATION AUTHORITY NONE	3. DISTRIBUTION/AVAILABILITY OF REPORT UNLIMITED
2b. DECLASSIFICATION/DOWNGRADING SCHEDULE NONE	
4. PERFORMING ORGANIZATION REPORT NUMBER(S) Technical Report #11	5. MONITORING ORGANIZATION REPORT NUMBER(S)
6a. NAME OF PERFORMING ORGANIZATION Stanford University	6b. OFFICE SYMBOL (If applicable)
7a. NAME OF MONITORING ORGANIZATION Office of Naval Research	
6c. ADDRESS (City, State, and ZIP Code) Department of Chemical Engineering Stanford University Stanford, CA 94305-5025	7b. ADDRESS (City, State, and ZIP Code) 800 North Quincy Avenue Arlington, VA 22217
8a. NAME OF FUNDING/SPONSORING ORGANIZATION Office of Naval Research	8b. OFFICE SYMBOL (If applicable)
9. PROCUREMENT INSTRUMENT IDENTIFICATION NUMBER N00014-87-K-0426	
8c. ADDRESS (City, State, and ZIP Code) 800 North Quincy Avenue Arlington, VA 22217	10. SOURCE OF FUNDING NUMBERS PROGRAM ELEMENT NO. / PROJECT NO. / TASK NO. / WORK UNIT ACCESSION NO.

11. TITLE (Include Security Classification)
Observation and Manipulation of Polymers by Scanning Tunneling and Atomic Force Microscopy

12. PERSONAL AUTHOR(S) M.M. Dovek, T.R. Albrecht, S.W.J. Kuan, C.A. Lang, R. Emch, P. Grütter, C.W. Frank, R.F.W. Pease, C.F. Quate

13a. TYPE OF REPORT	13b. TIME COVERED	14. DATE OF REPORT (Year, Month, Day)	15. PAGE COUNT
Technical	FROM _____ TO _____	88/7/13	20

16. SUPPLEMENTARY NOTATION
Submitted to J. Microscopy: Proceedings of STM 88

17. COSATI CODES		
FIELD	GROUP	SUB-GROUP

18. SUBJECT TERMS (Continue on reverse if necessary and identify by block number)

19. ABSTRACT (Continue on reverse if necessary and identify by block number)

The properties of monolayer films of organic materials are important for a variety of technologies. We have employed the STM and AFM to study Langmuir-Blodgett films of a variety of polymers on substrates of graphite, MoS_2, and Au(111) on mica. The polymers were poly(octadecyl acrylate) (PODA), atactic and syndiotactic poly(methyl methacrylate) (PMMA) and poly(2-methyl 1-pentene sulfone) (PMPS). One striking feature was the degree of order observed; a second was the morphological difference between films of submonolayer thickness (long thin fibrils) and those of at least monolayer thickness (lumpy structures arranged in domains). By pulsing the STM bias voltage to values in excess of 4 V, we were able to bring about local modification of the polymer morphology.

Keywords: Polymeric Films, Molybdenum Sulfate, Gold

20. DISTRIBUTION/AVAILABILITY OF ABSTRACT	21. ABSTRACT SECURITY CLASSIFICATION
☒ UNCLASSIFIED/UNLIMITED ☐ SAME AS RPT. ☐ DTIC USERS	Unclassified
22a. NAME OF RESPONSIBLE INDIVIDUAL Curtis W. Frank	22b. TELEPHONE (Include Area Code) 415-723-4573 / 22c. OFFICE SYMBOL

DD Form 1473, JUN 86 — Previous editions are obsolete. — SECURITY CLASSIFICATION OF THIS PAGE

cont'd pg 1

Observation and manipulation of polymers by scanning tunneling and atomic force microscopy

M.M. Dovek, T.R. Albrecht, S.W.J. Kuan†, C.A. Lang,

R. Emch, P. Grütter, C.W. Frank†, R.F.W. Pease*,

and C.F. Quate

Departments of Applied Physics,

†Chemical Engineering and *Electrical Engineering

Stanford University, Stanford, CA 94305

Abstract

The properties of monolayer films of organic materials are important for a variety of technologies. We have employed the STM and AFM to study Langmuir-Blodgett films of a variety of polymers on substrates of graphite, MoS_2, and Au(111) on mica. The polymers were poly(octadecyl acrylate) (PODA), atactic and syndiotactic poly(methyl methacrylate) (PMMA) and poly(2-methyl 1-pentene sulfone) (PMPS). One striking feature was the degree of order observed; a second was the morphological difference between films of submonolayer thickness (long thin fibrils) and those of at least monolayer thickness (lumpy structures arranged in domains). By pulsing the STM bias voltage to values in excess of 4 V, we were able to bring about local modification of the polymer morphology.

KEYWORDS: STM scanning tunneling microscopy, AFM atomic force microscopy, Langmuir-Blodgett Films, ultrathin films, polymers, acrylates, PODA poly(octadecyl acrylate), PMMA poly(methyl methacrylate), PMPS poly(methyl pentene sulfone), lithography, e-beam resist, side-chain crystalization.

I. INTRODUCTION

Direct imaging and manipulation of ultrathin organic films on solid surfaces is interesting for a variety of reasons. First of all, understanding the microstructure of these films is interesting for surface chemistry, biological applications, nanoscale fabrication and information recording. Furthermore, analysis of such images provides new information for understanding the contrast mechanism in STM and AFM imaging of adsorbed organic molecules, which has been an intriguing area of research since the conception of the instruments. (Smith *et al.* 1987, Foster & Frommer 1988, Marti *et al.* 1988)

The Langmuir-Blodgett (LB) technique can be used for preparing uniform layers of thin resist with very low pinhole densities. (Kuan 1988-1, Kuan 1988-2). We have utilized the LB technique with two different dipping geometries to prepare mono- and submonolayer films of poly(octadecylacrylate) (PODA), poly(methyl methacrylate) (PMMA), and poly (2-methyl 1-pentene sulfone) (PMPS) on graphite. MoS_2 and Au(111) on mica were also used as substrates for comparison.

PODA structures on graphite were imaged by both STM and AFM yielding identical morphologies. PMMA in its atactic and syndiotactic forms was imaged by STM; syndiotactic PMMA was found to give ordered structures under both dipping configurations. PMPS was imaged mainly for comparison of the writing thresholds.

It was possible to perform molecular manipulation of isolated polymer fibrils on graphite in the STM. A comparison was made between pulse polarities and between polymer types.

II. SAMPLE PREPARATION AND INSTRUMENTATION

The LB films were atactic PODA with a weight average molecular weight (M_w) of 23,300 and number average molecular weight of 13,000 (M_n), syndiotactic PMMA, with M_w=100,000, and PMPS . The monomer repeat units of each of these polymers as well the stereochemical structure of atactic and syndiotactic PMMA are shown in Figure 1.

The LB films were prepared by horizontally lifting the substrate out of the trough or by dipping the sample vertically into the water subphase and lifting it vertically out. This procedure is described in more detail elsewhere (Albrecht *et al.* 1988-2) . The presence of the film was checked by ellipsometry.

The STM and the AFM were both operated in air in the current imaging mode. The STM feedback bandwidth, however, was set to approximately twice the line scan rate. The contrast information was again derived from the current error signal. Bias voltages in the vicinity of 0.6 V were used and the tunneling current was kept lower than 0.5 nA. A more detailed description of the STM and AFM instrumentation can be found elsewhere. (Bryant *et al.* 1986, Albrecht and Quate 1987, Albrecht *et al.* 1988-2)

III. FILM MORPHOLOGY OBSERVED BY STM AND AFM

One common feature that was observed on all samples with the two dipping configurations was the fact that the image contained parallel chains of varying densities depending on the deposition. The chains remained parallel over very large areas. It was suggested that the polymer chains become stretched during the initial spreading of the

chloroform solution as the Langmuir film is formed on the water surface (Wissbrun 1988).

On samples that were prepared by horizontal dipping, we observed submonolayer coverages of PODA with the STM. There were several areas of bare graphite with isolated fibrils extending in length from one hundred to several hundred Angstroms with the graphite background clearly visible on either side. Figure 2 (a) shows an isolated narrow fibril and the graphite lattice background used for geometric calibration. The fibril width was 8 ± 2 Å with the shadow to the right of the fibril being caused by high pass filtering and the delayed response of the feedback due to the strong current signal. When the scan speed was reduced further, the tip response varied between 5 and 10 Å on these isolated fibrils with respect to the background while the feedback maintained contours of constant current. The graphite lattices on the left and on the right of the fibril are in registry. Steps and grain boundaries on graphite are very rarely observed and are easy to discriminate against. (Albrecht *et al.* 1988-1) We can, therefore, definitely exclude the possibility that the observed fibrils could be due to steps or grain boundaries.

Figure 2 (b) shows a parallel array of fibrils. We observed identical morphologies on the sample prepared by horizontal lifting when analyzed with the AFM. Figures 2 (c) and 2 (d) are corresponding AFM images of the morphologies observed by the STM shown in Figures 2 (a) and (b).

In the horizontally prepared sample, we observed an isolated highly ordered region of approximately 300 Å x 300 Å, shown in Figure 3. The spacing between rows is one to two times the side chain length. This spacing agrees with a two dimensional version of a model proposed for the crystalline bulk. (Plate *et al.* 1971, Albrecht *et al.* 1988-2). This same structure was also observed on PODA deposited on Au (111) on mica (Emch *et al.*

1988). The 20 Å periodicity that is observed along the backbone could reflect side chain interactions or even crystallization as is typically observed in bulk PODA. (Hsieh *et al.* 1976)

The second polymer whose morphology we studied was syndiotactic PMMA. Sample preparation was again done by two dipping methods. The first dipping method yielded isolated chains and clusters of parallel chains as was observed with PODA with occasional twists and kinks in the chains of up to 45 degrees. One possible explanation for why one would observe kinks in PMMA and not in PODA, is the fact that the strong long side chain interactions in PODA keep the backbone straight over much longer distances.

PMMA samples that were prepared by vertical dipping, on the other hand, demonstrated several hundred Angstrom sized domains of parallel polymer fibrils. Figure 4 (a) shows a 500 Å x 500 Å region showing three different domains and a step down to graphite. Figure 4 (b) is a 200 Å x 200 Å zoom into the domain at the center of Fig 4 (a). The parallel fibrils are separated by 15 Å.

IV. POLYMER MODIFICATION WITH THE STM

The samples that were used for this experiment were PODA and PMPS samples prepared by the horizontal raising technique. A rectangular voltage pulse of 100 ns duration was applied to the STM tip as it was scanned over part of the isolated chain.

Figure 5 (a) is a 400 Å x 400 Å image showing a bundle of fibrils before a pulse is applied to the tip. Figure 5 (b) shows the same area after the pulse. The pulse disrupts the highly parallel structure over a 50 Å radius and appears to have broken the fibril where the pulse is applied. The threshold for writing seems to vary from tip to tip and position on the

sample and was found to be around 4 V. These marks were produced by pulses of either polarity.

In order to investigate whether the disruption can be explained by the breaking of the backbone, we repeated the same experiment with PMPS whose backbone contains two C-S bonds per repeat unit. The C-S bond energy is 2.9 eV whereas the C-C bond energy is 3.8 eV. If the marks are due to the breaking of the backbone, one would expect lower voltage thresholds for PMPS. We found the threshold voltage to be slightly lower compared to PODA, but the difference is not as large as the one to be expected from the bond energy difference.

We induced similar morphological changes on the PMPS. Figure 6 (a)-(d) shows a time sequence corresponding to a single pulse. In figure 6 (a) we see a parallel cluster of chains. Figure 6 (b) is shown a couple seconds after the pulse. Figures 6 (c) and 6 (d) are taken 10 and 20 seconds after the pulse respectively and illustrate the time evolution of the mark induced by the voltage pulse. The feature size is again less than 100 Å x 100 Å.

In order to investigate what would happen if we pulsed on a region without apparent fibrils, we applied four pulses in a rectangular pattern of dots. The results are shown in Figure 7. The feature size is around 30 Å x 30 Å. A similar method for writing single dots of 10 Å, was previously illustrated for the STM on a dimethyl phthlate (DMP) covered graphite surface. (Foster *et al.* 1988) The use of commonly present hydrocarbons as "contamination resist" for an electron beam had previously been demonstrated resulting in 80 Å metallic features. (Broers *et al.* 1976). Contamination had also been used to produce sub 0.1 μm lines in an STM for subsequent inspection with a Scanning Electron Microscope. (McCord and Pease 1986)

One possible explanation for the 4 eV threshold would be that it corresponds to the barrier height for generating free electrons in the gap. The lower effective barrier heights that have been reported in air do not contradict this, as they are mainly due to contamination mediated deformations (Mamin *et al.* 1986, Lang and Dovek 1988).

The hydrocarbon density is larger when the tip is over a bundle of polymers due to the polymer backbone, its side chains, the commonly present hydrocarbons and additionally attracted ones. Since the feature size observed in these areas is larger than features formed on bare areas, this suggests that the writing mechanism involves the breaking and reformation of intramolecular and surface bonds.

V. CONCLUSIONS

LB deposited PODA, atactic-PMMA, syndiotactic-PMMA and PMPS have been imaged on graphite using two powerful tools: STM and AFM. These results give us information about the morphology of these films. The surface coverage was found to be in agreement with the deposition geometry used. Domain sizes were found to be smaller in PMMA than PODA possibly due to reduced side chain length. Furthermore, we have demonstrated a mechanism for marking these polymers with the STM that seems to be similar in nature to e-beam lithography on acrylates and contamination resist.

ACKNOWLEDGEMENTS

The authors would like to thank A.W. Moore for providing the HOPG, A.S. Gozdz at Bell Communications Research for providing the PMPS, L. Lacomb for his help with image processing, and M. Kirk and J. Foster for useful discussions. We acknowledge the support of an IBM Predoctoral Manufacturing Fellowship (MMD), a National Science Foundation Graduate Fellowship (TRA), and a German National Scholarship Foundation overseas fellowship (CAL). This project was supported by the Defense Advanced Research Projects Agency, the Office of Naval Research N00014-87-K-0426, and the National Science Foundation ECS 86-08318.

REFERENCES

T.R. Albrecht and C.F. Quate (1987) Atomic resolution imaging of a nonconductor by atomic force microscopy. *J. Appl. Phys.* **62**, 2599-2602.

T.R. Albrecht, H.A. Mizes, J. Nogami, S.I. Park, and C.F. Quate (1988) Observation of tilt boundaries in graphite by scanning tunneling microscopy and associated multiple tip effects. *Appl. Phys. Lett.* **52**, 362-264.

T.R. Albrecht, M.M. Dovek, C.A. Lang, P. Grütter, C.F. Quate, S.W.J. Kuan, C.W. Frank, and R.F.W. Pease (1988) Imaging and Modification of Polymers by Scanning Tunneling and Atomic Force Microscopy. *J. Appl. Phys.* **64**, xxxx.

A.N. Broers, W.W. Molzen, J.J. Cuomo, and N.D. Wittels (1976) Electron Beam Fabrication of 80-Å metal structures. *Appl. Phys. Lett.* **29**, 596-598.

A. Bryant, D.P.E. Smith, and C.F.Quate (1986) Imaging in real time with the tunneling microscope. *Appl. Phys. Lett.* **48**, 832-834.

R. Emch, J. Nogami, M.M.Dovek, C.A. Lang and C.F. Quate (1988) Characterization of gold surfaces for use as substrates in scanning tunneling microscopy studies. submitted to *J. Appl. Phys.*

J.S. Foster, and J.E. Frommer (1988) Imaging of liquid crystals using a tunneling microscope. *Nature* **333**, 542-545.

J.S. Foster, J.E. Frommer, and P.C. Arnett (1988) Molecular manipulation using a tunneling microscope. *Nature* **331**, 324-326.

H.W.S. Hsieh, B.Post, and H. Morawetz (1976) A Crystallographic Study of Polymers Exhibiting Side-Chain Crystallization. *J. of Polymer Science* **14**, 1241-1255.

S.W.J. Kuan, C.C. Fu, D..R. Allee, P. Maccagno, R.F.W. Pease, and C.W. Frank (1988) Ultrathin Polymer Films for Microlithography. submitted to *J. Vac. Sci. Technol.*

S.W.J. Kuan, C.C. Fu, R.F.W. Pease and C.W. Frank (1988) Studies of Ultrathin Polymer Films for lithographic applications. to be published in *Proceedings of SPIE, Symposium of Microlithography.*

C. A. Lang and M. M. Dovek, unpublished.

H.J. Mamin, E. Ganz, D.W. Abraham, R.E. Thomson, and J. Clarke (1986) Contamination-mediated deformation of graphite by the scanning tunneling microscope. *Phys. Rev. B* **34**, 9015-9018.

O. Marti, H.O. Ribi, B. Drake, T.R. Albrecht, C.F. Quate, and P.K. Hansma (1988) Atomic Force Microscopy of an Organic Monolayer. *Science* **239**, 50-52.

M.A. McCord and R.F.W. Pease (1986) Lithography with the scanning tunneling microscope. *J. Vac. Sci. Technol. B* **4**, 86-88.

N.A. Plate, V.P. Shibaev, B.S. Petrukhin, Y.A. Zubov, and V.A. Kargin (1971) Structure of Crystalline Polymers with Unbranched Long Side Chains. *J. of Polymer Science* **9**, 2291-2298.

D.P.E. Smith, A. Bryant, C.F. Quate, J.P. Rabe, Ch. Gerber, and J.D. Swalen (1987) Images of a lipid bilayer at molecular resolution by scanning tunneling microscopy. *Proc. Natl. Acad. Sci.* **84**, 969-972.

K. Wissbrun, Hoechst Celanese, private communication.

FIGURE CAPTIONS

Figure 1 Structures of (a) PODA, (b) PMMA and (c) PMPS monomer units. Stereochemical structures of (d) atactic and (e) syndiotactic PMMA.

Figure 2 STM and AFM images of PODA submonolayers on graphite: (a) An isolated fibril on the otherwise clean graphite seen by STM (75 Å x 75 Å); (b) larger parallel fibrils in other areas seen by STM (440 Å x 440 Å); (c) An isolated fibril stretched across the surface seen by AFM (60 Å x 60 Å); (d) parallel fibrils seen by AFM (380 Å x 380 Å).

Figure 3 An STM image of a two dimensional ordered overlayer suggestive of bulk ordering (300 Å x 300 Å).

Figure 4 STM Images of monolayer coverage syndiotactic-PMMA: (a) An area showing a few domains of parallel chains and a step down to graphite (500 Å x 500 Å), (b) a 200 Å x 200 Å blowup of one of the domains of Fig 4 (a).

Figure 5 Modification of PODA with the STM: (a) a wide fibril before a pulse is applied to the tip, (b) the same area after the pulse (400 Å x 400 Å).

Figure 6 Modification of PMPS with the STM: (a) a wide fibril before a pulse is applied to the tip, (b) the fibril immediately after the pulse, same area (c) 10 seconds and (d) 20 seconds after the pulse. The image size is 450Å x 450Å.

Figure 7 Writing on an uncovered area. (200 Å x 200 Å). A 4 Volt pulse was applied to the tip at the corners of the shown quadrilateral.

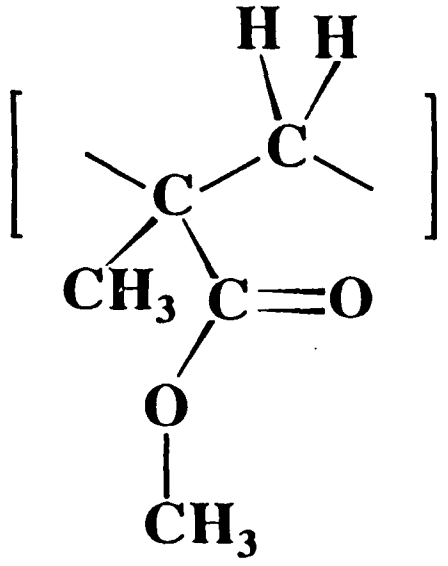

PMMA

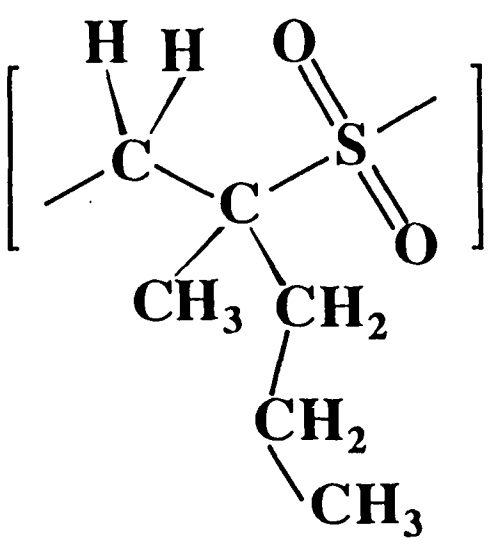

PMPS

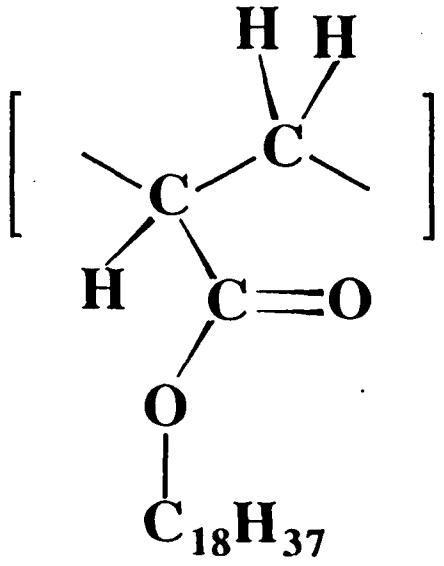

PODA

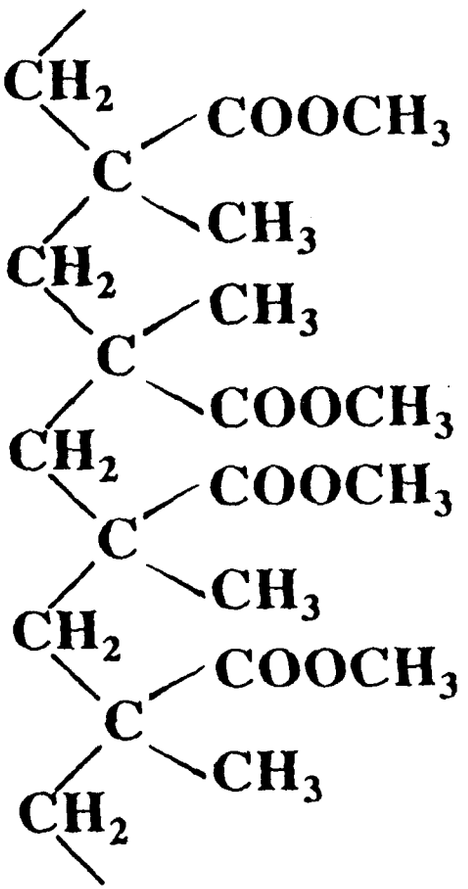

atactic

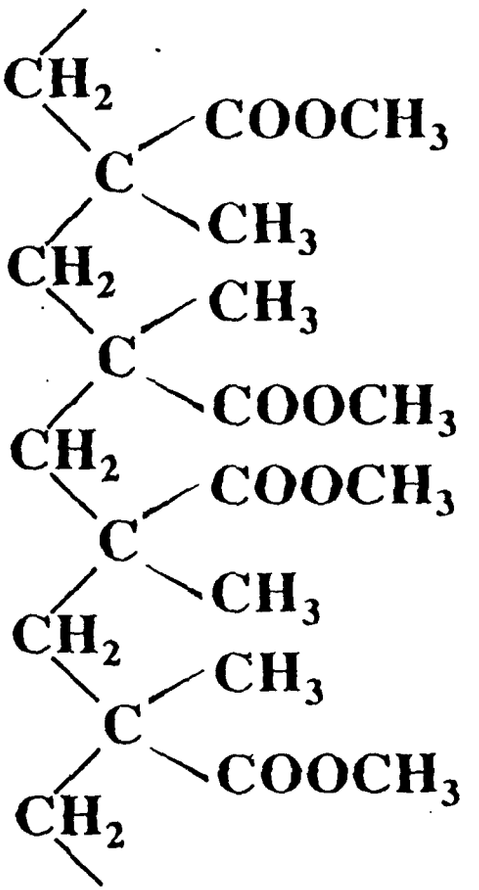

syndiotactic

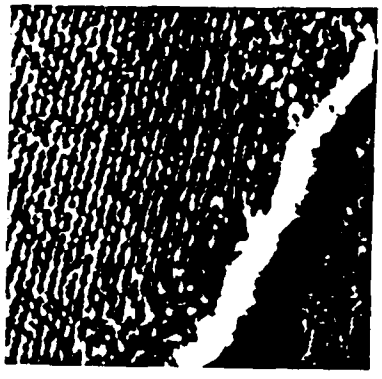

a

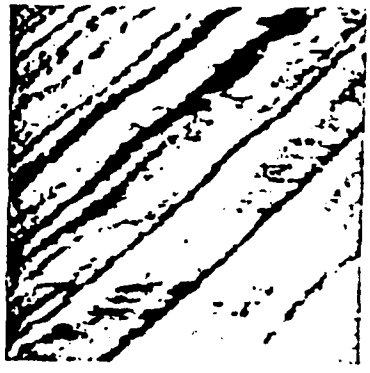

b

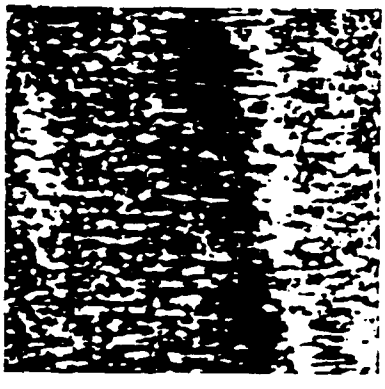

c

d

Fig. 2

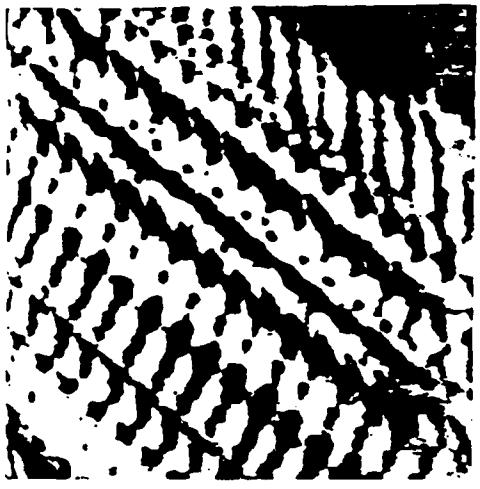

Fig. 3

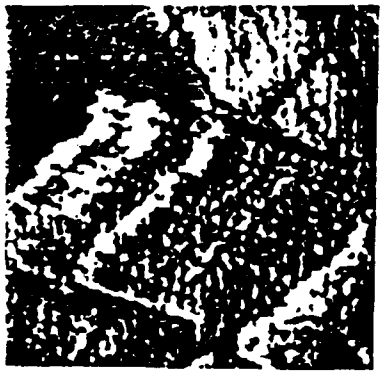

a

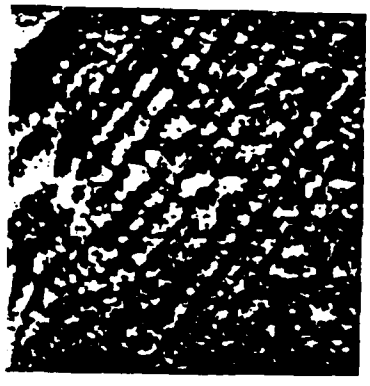

b

Fig. 4

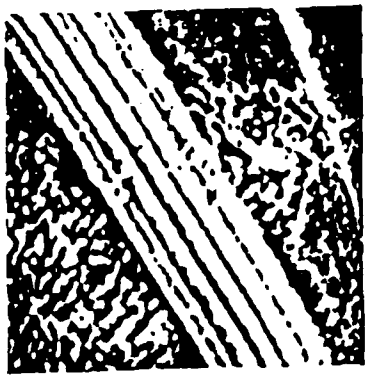

a

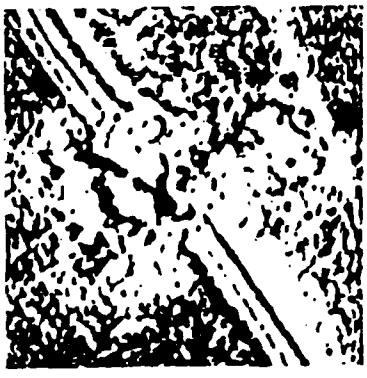

b

Fig. 5

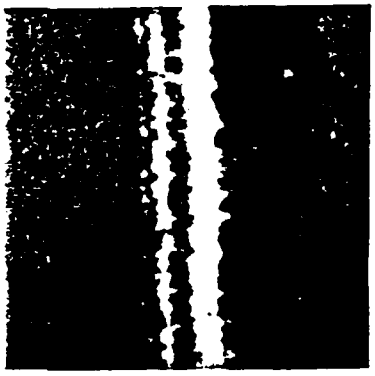

a

b

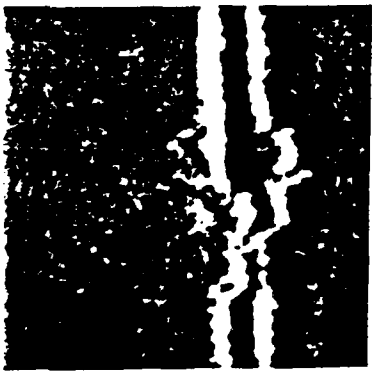

c

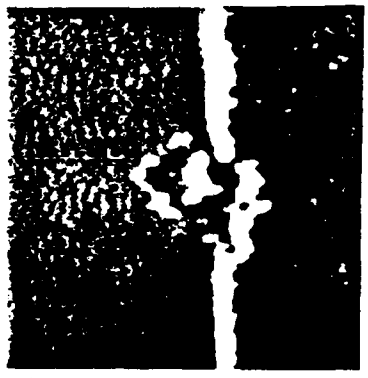

d

Fig. 6

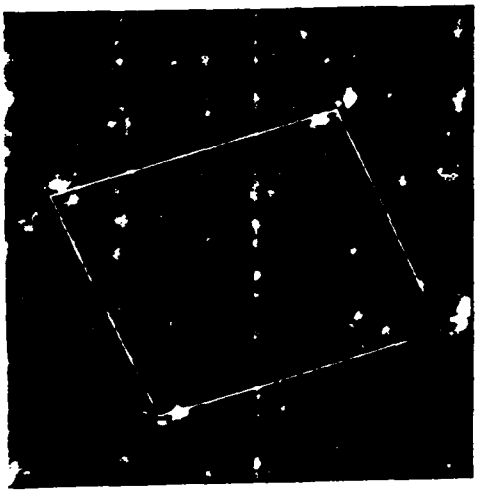

Fig. 7